Supporting Information

Reaction of chloroauric acid with histidine in microdroplets yields catalytic Au-$(His)_2$ complex

Kai Luo[a, ‡], Jia Li[a, ‡], Yufei Cao[b], Chengyuan Liu[a], Jun Ge[b], Hao Chen [c], Richard N. Zare[a,*]

[a] Department of Chemistry, Fudan University, Jiangwan Campus, Shanghai 200438, China

[b] Key Lab for Industrial Biocatalysis, Ministry of Education, Department of Chemical Engineering, Tsinghua University, Beijing 100084, China

[c] Department of Chemistry and Environmental Science, New Jersey Institute of Technology, Newark, NJ 07102, USA

*Correspondence should be addressed to Richard N. Zare; Email: rnz@fudan.edu.cn

1. General information

High-angle annular dark-field scanning transmission electron microscopy (HAADF-STEM) was recorded on a JEOL JEM-2100F Instrument operated at 200 kV.

The X-ray photoelectron spectroscopy (XPS) analysis was performed on a Thermal Scientific ESCALAB 250 Xi instrument using an monochromatized Al K_α X-ray source (E = 1486.6 eV) operated at 15 kV and 15 mA.

The high-performance liquid chromatography (HPLC) analysis was performed on an Agilent 1260 series with diode array detector (DAD). The 20 μL reaction solution was injected by an automatic sampler and analysis by Agilent TC-C18 column (150 mm×4.6 mm, 5 μm) with the detection wavelength of 214 nm. The mobile phase was composed by the ACN-H_2O with the mode of gradient elution (0-3 min with 5% ACN for 2 min, then 5-95% ACN for 5-15 min and finally kept for 5 min).

Cyclic voltammetry (CV) measurements were carried out using a Chi 760i Potentiostation Instrument (Chi Instruments, China) potentiostat. All measurements were conducted using a screen-printed three-electrode configurations consisting of a platinum geometric working electrode area of 3 mm diameter, counter electrode, and Ag/AgCl reference. Connectors for the efficient connection of the screen-printed electrochemical sensors were purchased from Kanichi Research Services Ltd. The scan range was conducted form -2.0 V to +2.0 V with scan rate of 0.1 $V \cdot s^{-1}$.

The fluorescence (FL) spectrum was performed on the Agilent Cary Eclpse Fluorescence Spectrophotometer (Aiglet, USA) with the E_x and E_m of 396 nm and 495 nm, respectively.

Nuclear magnetic resonance spectrum (^{1}H-NMR) was recorded on an AVANCE III HD 400 MHz (Bruker, USA) with D_2O for Au-$(His)_2$ and $DCCl_3$ for product of the enamine reaction.

2. Experimental

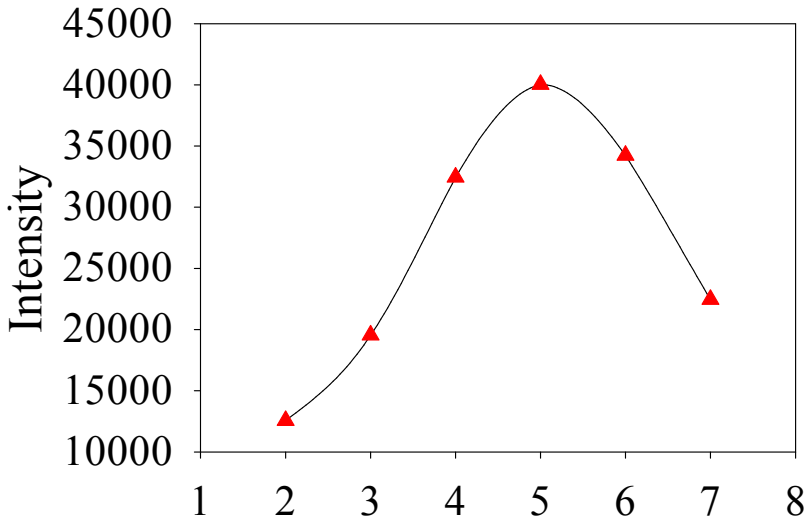

Figure S1 The peak intensity at *m/z* of 964.9904 as a function of travel distance from the tip of sprayer to the inlet of the mass spectrometer. This is the behavior of just one of the ions in this mass range.

As expected, the negative-ion ESI mass spectra of Au_5 clusters are comprised of a series of peaks associated with multiply charged anions formulated as $[Au_n(L)_m\text{-}xH]^{y-}$, where n, m, x and y represents the numbers of gold atoms, ligands, dissociated protons and charges, respectively.[1]

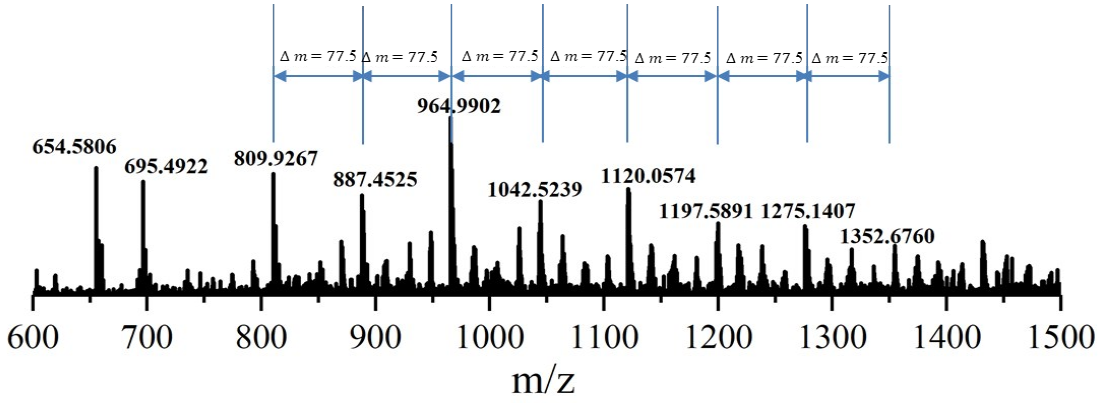

Figure S2. Enlarged mass spectra from the homemade ESSI apparatus of gold clusters from *m/z* = 600 to 1500. The arrows indicate peak related to Au_5 clusters encapsulated by different number of histidine with mass spacing of 77.5 Da. The peaks of 654.5 and 732.4 correspond to Au_5His_1 and Au_5His_2, respectively, although the latter is less certain because of the weak intensity. We speculate that the peak at the *m/z* of 695.5 is the ion of $[Au+3(His)+Cl]^-$, which fits to Au-$(His)_2$ (*m/z* 505) with Cl^- (*m/z* 35) and another His (*m/z* 155). This assignment is further verified by the isotopic ratio of 3:1 with the *m/z* of 695.5 and 697.5.

Table S1 The composition of Au_5 clusters with the different number of histidine molecules (number.:3-10) and the corresponding mass-to-charge ratio with two negative charges.

m/z		M.F.	M.E.	m/z		M.F.	M.E.
Ther.	Meas.		(ppm)	Ther.	Meas.		(ppm)
809.9231	809.9267	$[Au_5(His)_3\text{-}5H+5Cl]^{2-}$	4.4	1120.0621	1120.0574	$[Au_5(His)_7\text{-}5H+5Cl]^{2-}$	4.2
887.4579	887.4525	$[Au_5(His)_4\text{-}5H+5Cl]^{2-}$	6.1	1197.5969	1197.5891	$[Au_5(His)_8\text{-}5H+5Cl]^{2-}$	6.5
964.9927	964.9902	$[Au_5(His)_5\text{-}5H+5Cl]^{2-}$	2.6	1275.1316	1275.1407	$[Au_5(His)_9\text{-}5H+5Cl]^{2-}$	7.1
1042.5274	1042.5239	$[Au_5(His)_6\text{-}5H+5Cl]^{2-}$	3.4	1352.6664	1352.6760	$[Au_5(His)_{10}\text{-}5H+5Cl]^{2-}$	7.1

"M.F."-denote for the molecular formula

"M.E"- denote for the mass error

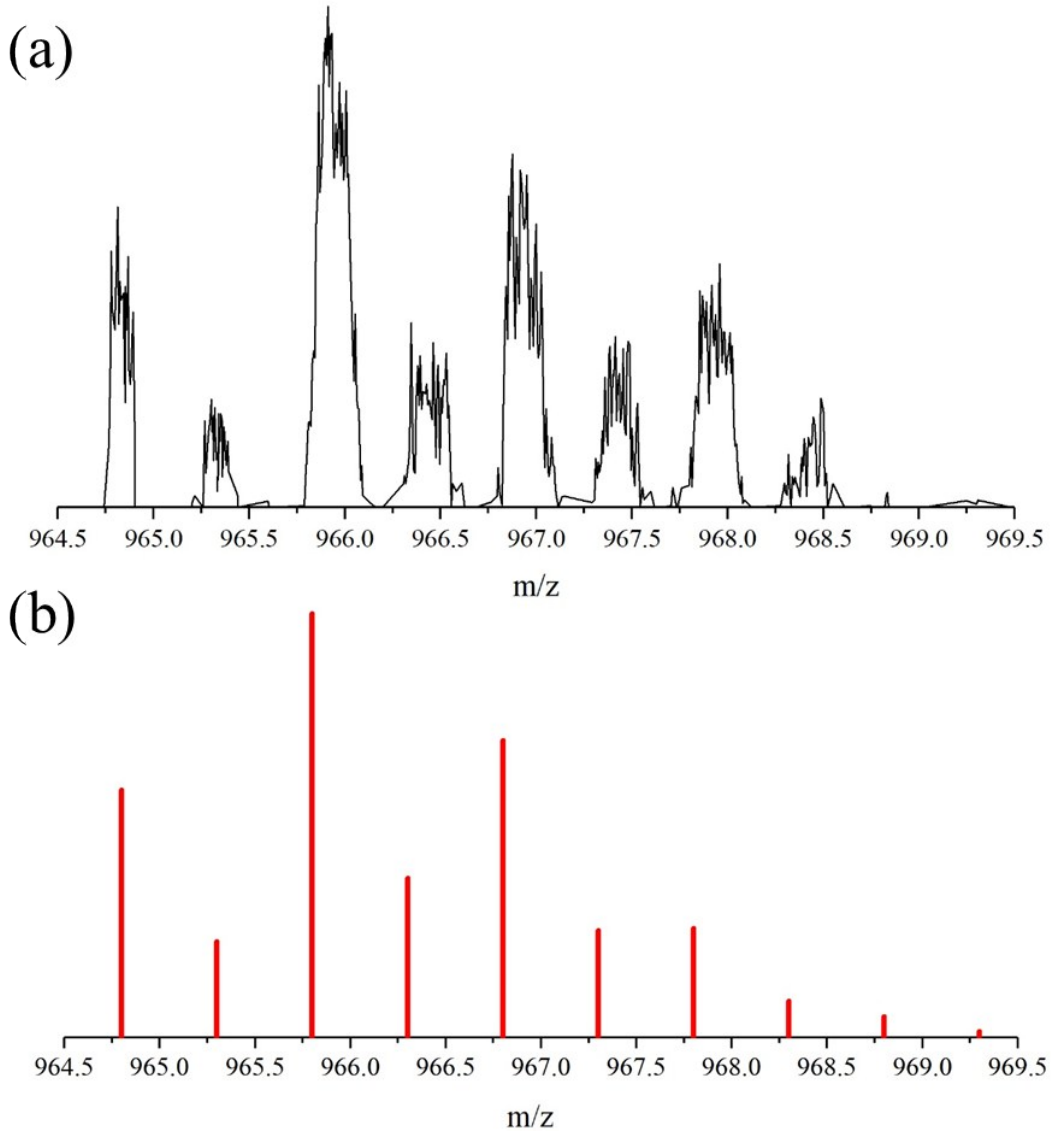

Figure S3 Mass spectrum of Au_5 clusters, (a) which is composed by $[Au_5(His)_5\text{-}5H+5Cl]^{2-}$ and (b) the theoretical simulated isotope peaks.

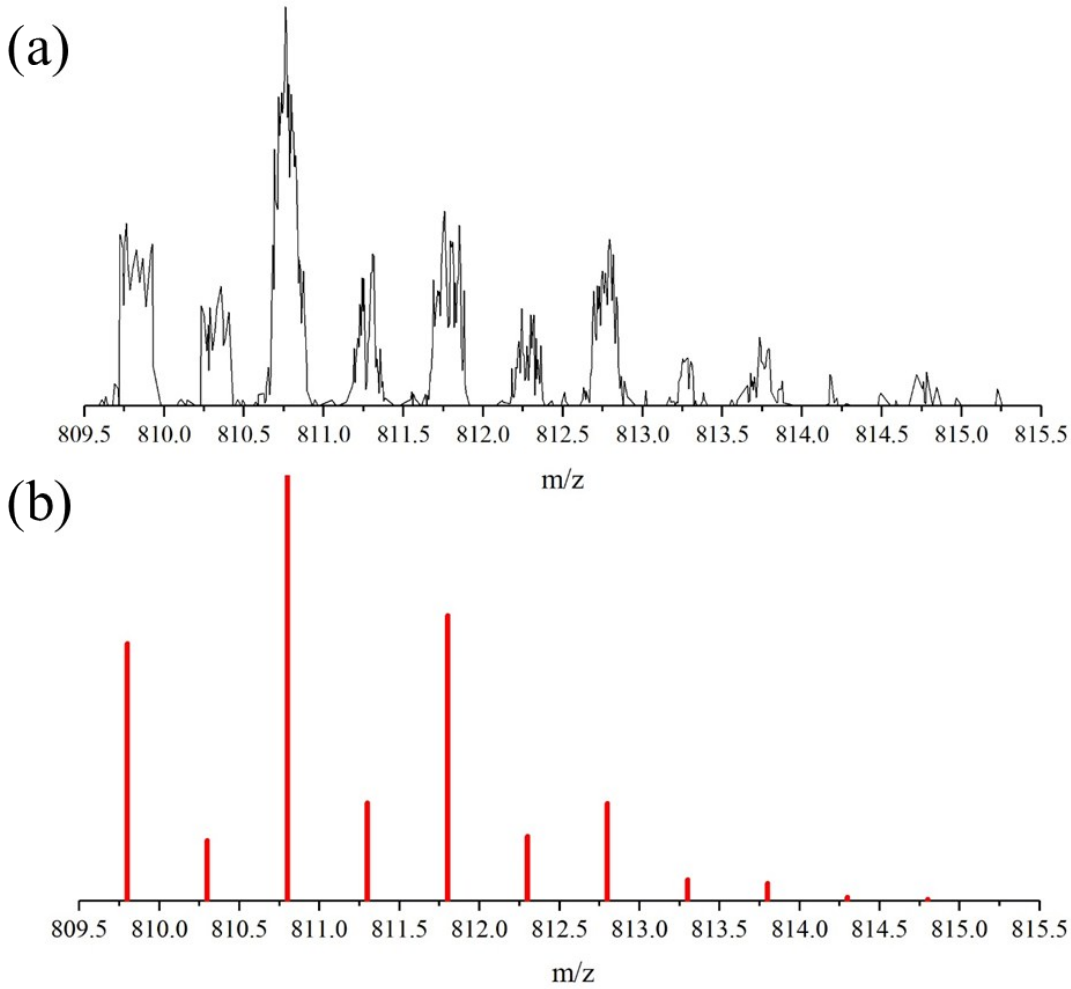

Figure S4 Mass spectrum of Au_5 clusters, (a) which is composed by $[Au_5(His)_3\text{-}5H+5Cl]^{2-}$ and (b) the theoretical simulated isotope peaks.

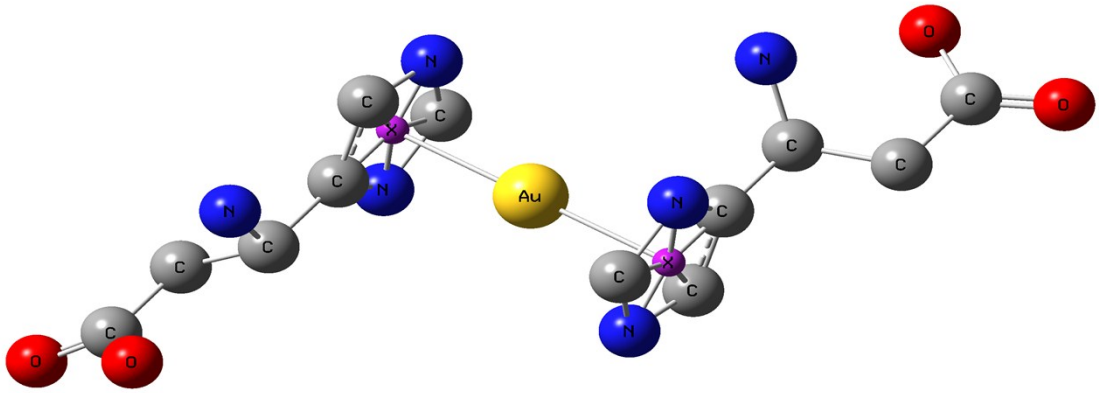

Figure S5 The image of Au-$(His)_2$. The Au atom connects to the center of imidazole, similar to the structure of ferrocene.

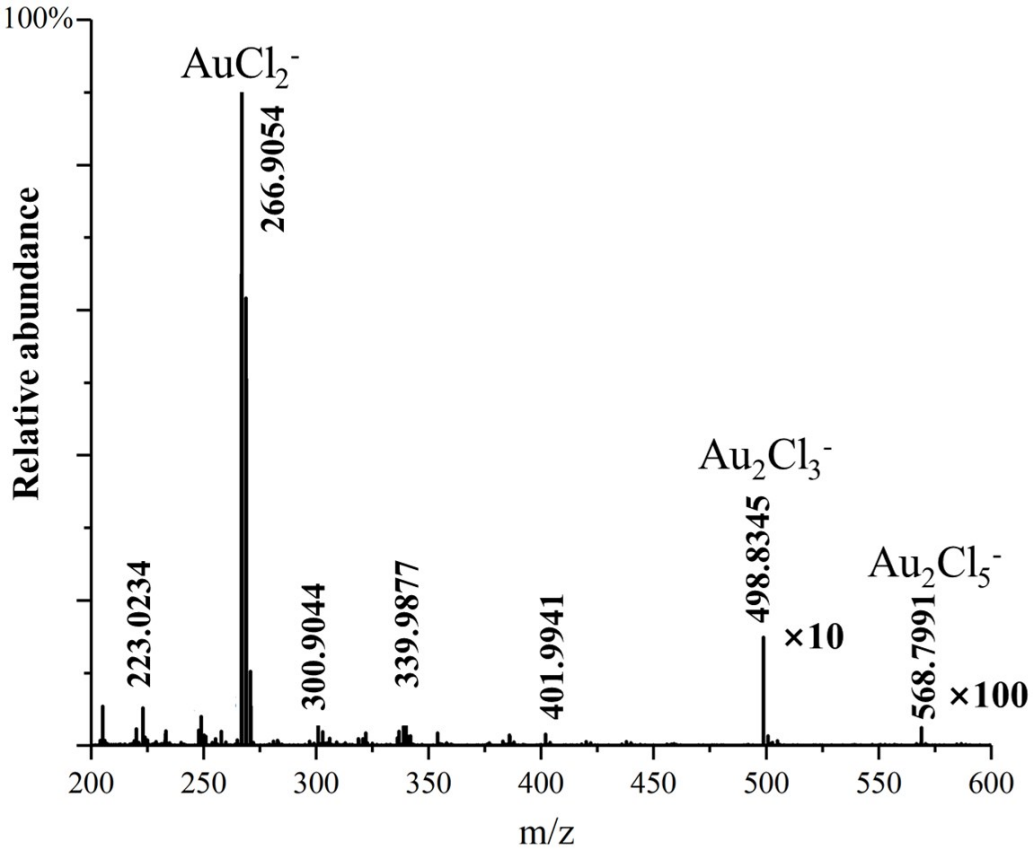

Figure S6 Mass spectrum of 100 μM $HAuCl_4$ solution in H_2O sprayed in forms of microdroplets with a negative high voltage of 4.5 kV. The *m/z* peaks for both the original $AuCl_4$ (oxidation number +3) and the reduced species, $Au_2Cl_3^-$ (+1), $AuCl_2^-$ (+1), and $Au_2Cl_4^-$ (+2) were observed.

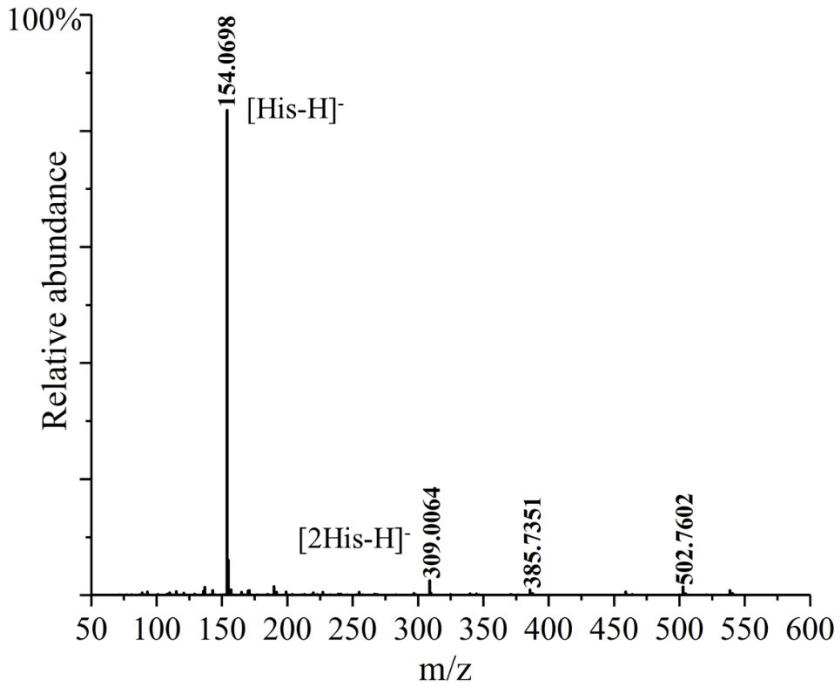

Figure S7 Mass spectrum of 100 μM $AuCl_3$ and 1000 μM Histidine in H_2O sprayed in forms of microdroplets with a negative high voltage of 4.5 kV.

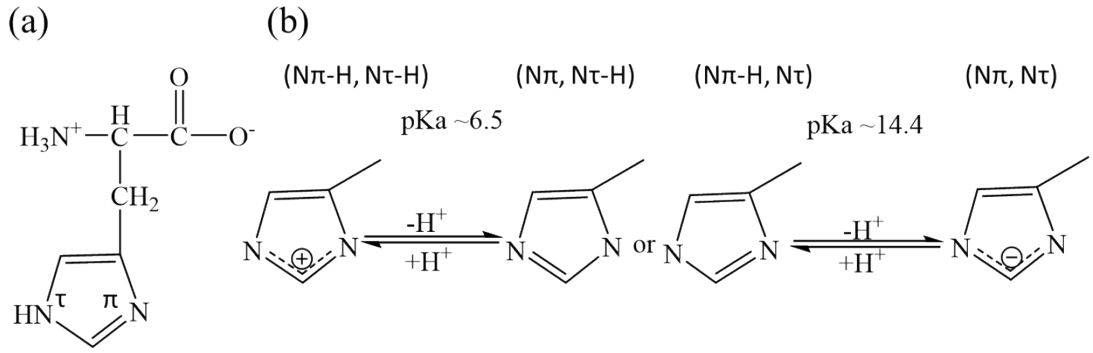

Figure S8 Chemical structure of the amino acid histidine (His) under physiological conditions (pH ≈ 7.5), (a) where '***π***' denote as the 'pyridine-like' nitrogen atom and '***τ***' denote as the 'pyrrole-like' nitrogen atom (b) Depending on pH and other solution conditions, the histidine imidazole side chain can exist in a number of forms.

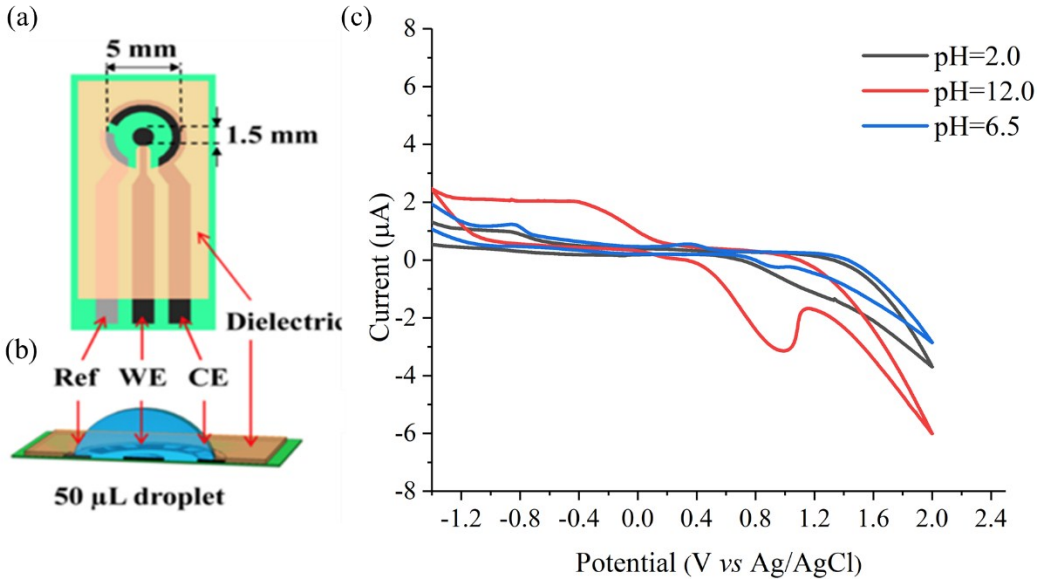

Figure S9 The setup of screen printing electrode[2] (a) with 50 µL droplet of water solution with $HAuCl_4$ (100 µM) and histidine (100 µM) (b) and the recorded corresponding CVs (v = 0.1 V/s), (c) where 'black', 'red' and 'blue' in the CV curves represent the pH of 2.0, 12.0 and 6.5, respectively.

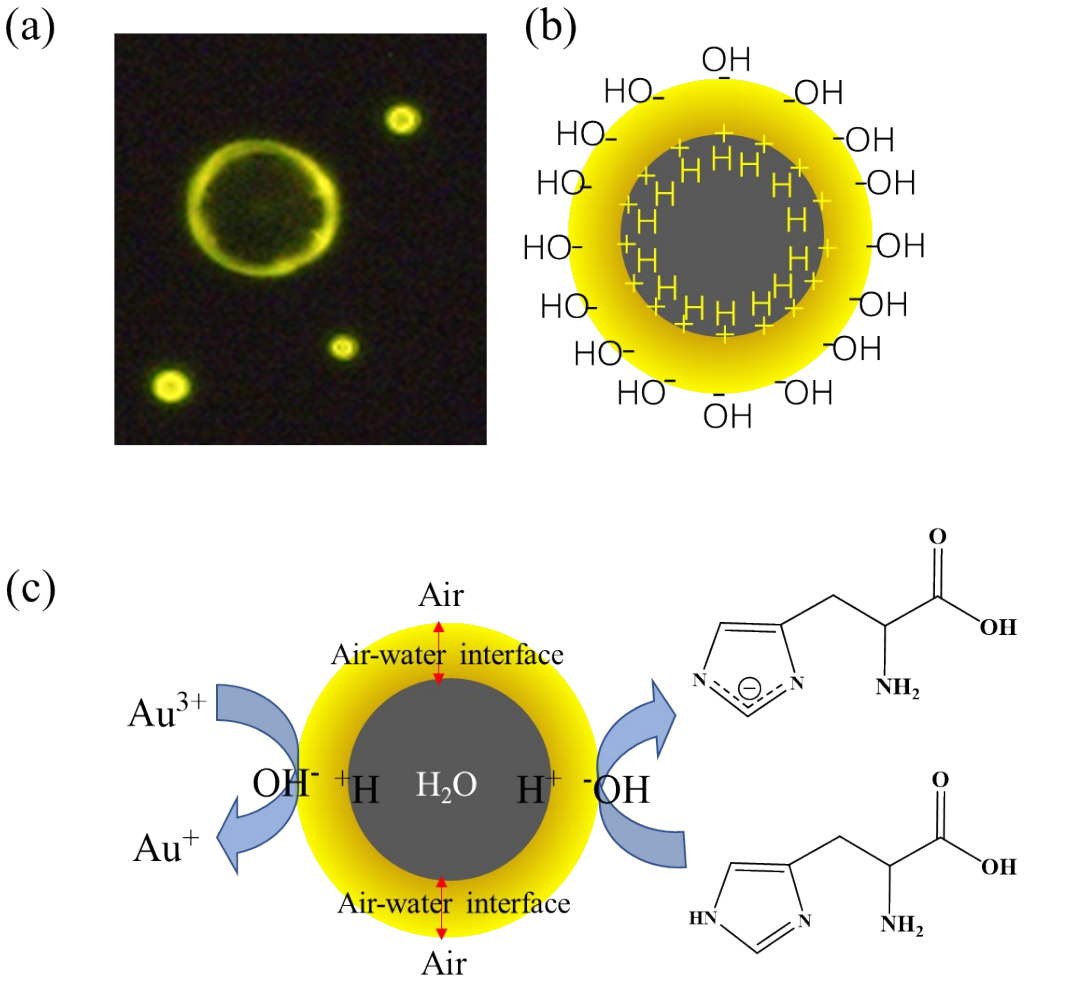

Figure S10 (a) The FL image of microdroplet (particle size=8 μm) of $HAuCl_4$ (100 μM) and histidine (100 μM) water solution was captured by fluorescence confocal microscopy and (b) the simulating double layer formed at the air-water interface of the microdroplet and (c) the possible mechanism for the formation of Au^+ and NHC ligand at the air-water interface.

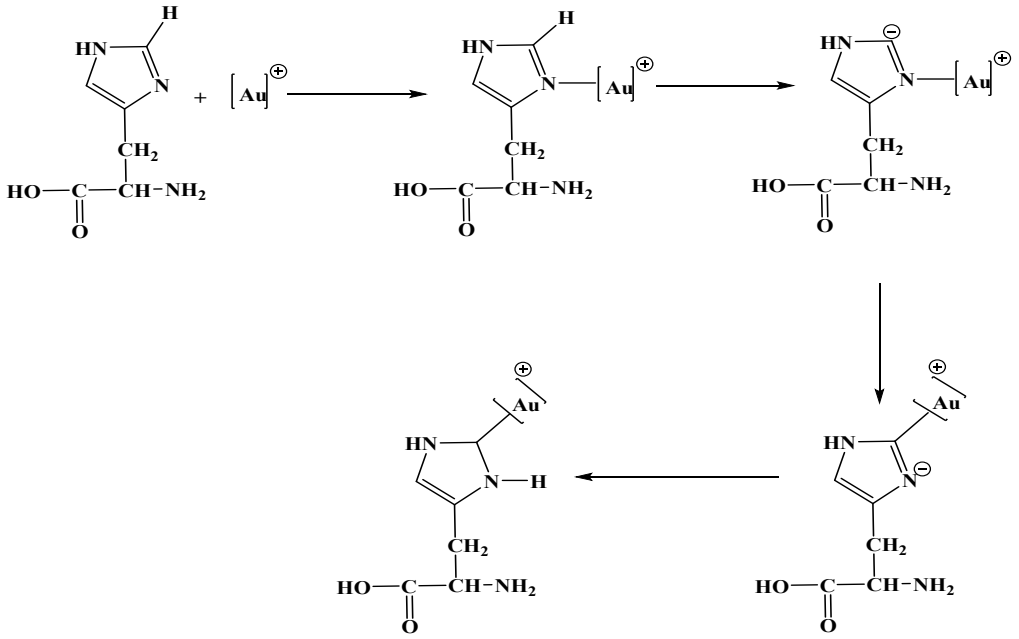

Figure S11 The detail possible mechanism[3] for the formation of Au^{+} and NHC ligand at the air-water interface.

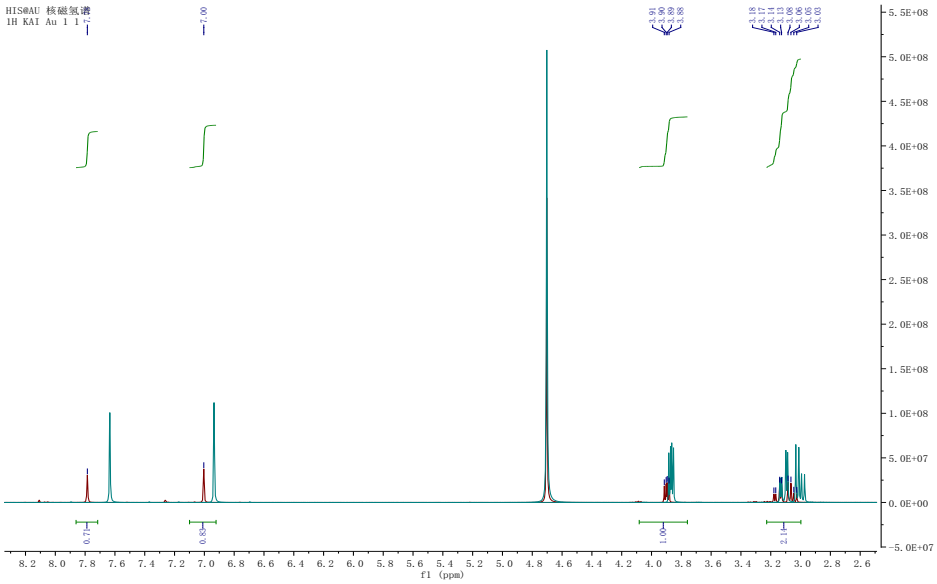

Figure S12 ^{1}H NMR result for histidine (green) and Au-$(His)_2$ (red), which means that the electron cloud density of imidazole ring of the complex decreased and formed a large π bond conjugated system. The largest peak is the proton signal from HOD arising from residual H_2O in the sample.

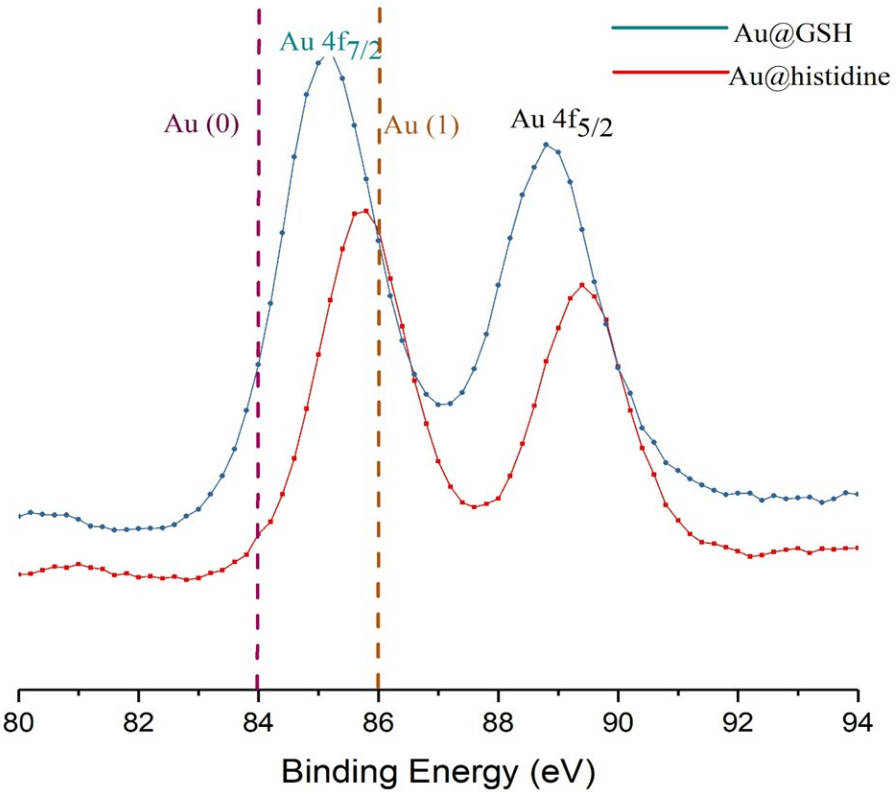

Figure S13 The XPS result showed that the Au-$(His)_2$ complexes mainly exist in the form of 1 valence, which is different from zero valence in gold nanoclusters, Au@GSH (green) and Au-$(His)_2$ (red)

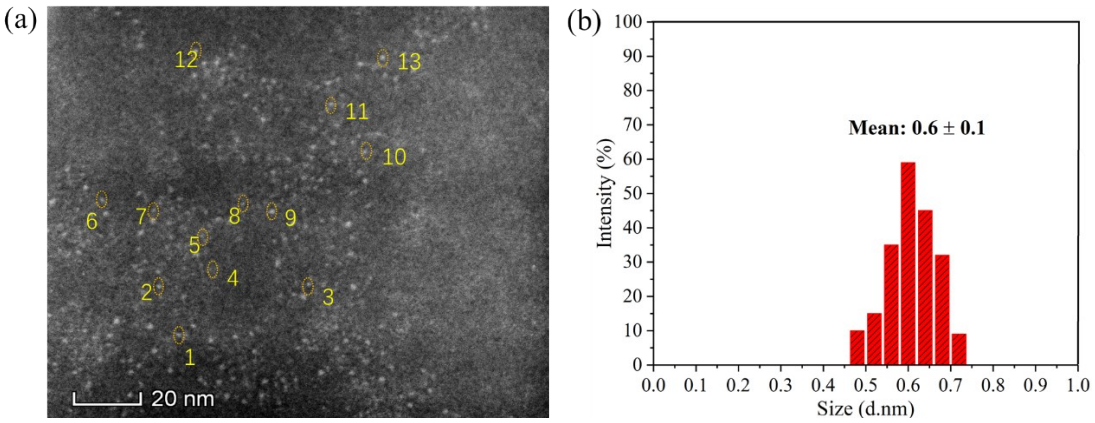

Figure S14 HAADF-STEM of 0.6 nm Au-$(His)_2$. (a) HAADF-STEM image of 0.6 nm Au-$(His)_2$ and (b) the corresponding size distribution that calculated by the software of Nano Measurer 1.2. The standard deviations were calculated from 13 particles

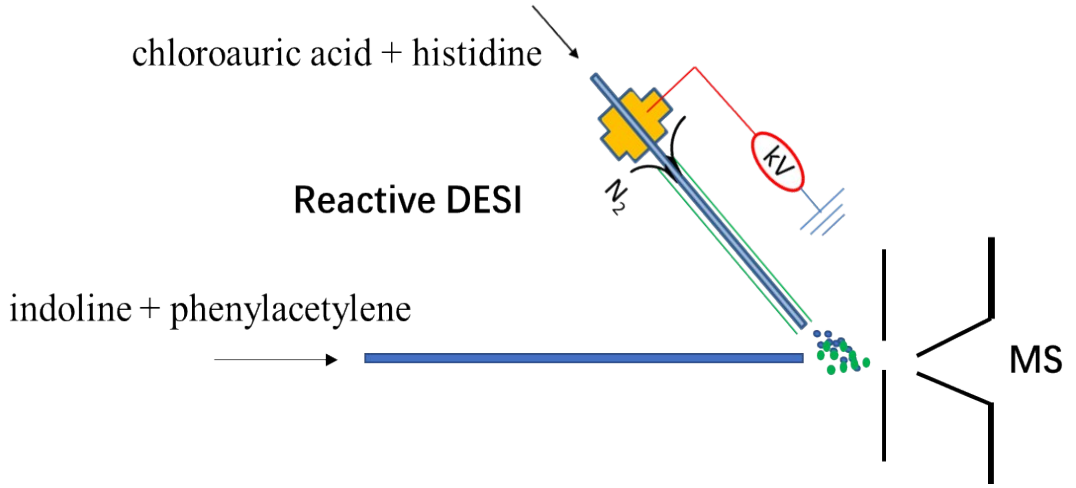

Figure S15 Online reactive DESI-MS setup upon spraying the solution of $HAuCl_4$ (10 μM) and His (100 μM) in water mixed with phenylacetylene (100 μM), and indoline (100 μM) in acetonitrile solution with the high voltage of +4.5 kV.

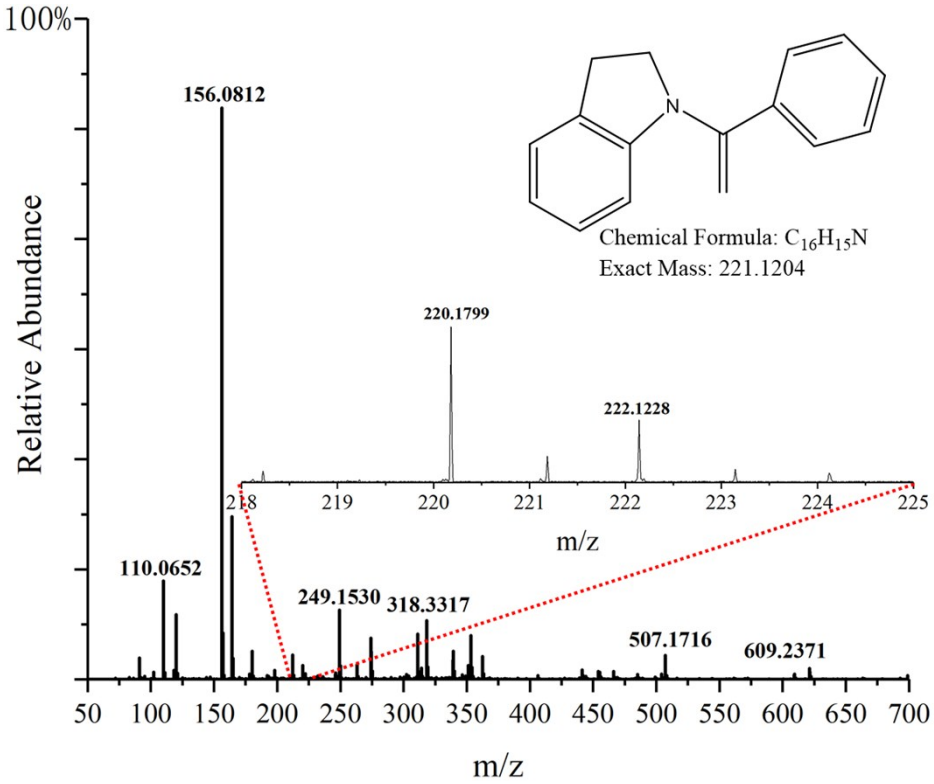

Figure S16 Online reactive DESI-MS spectra upon spraying the solution of $HAuCl_4$ (10 μM) and His (100 μM) in water mixed with phenylacetylene (100 μM), and indoline (100 μM) in acetonitrile solution with the high voltage of +4.5 kV. The inset shows the zoomed-in intermediate ion produced by the reactive DESI.

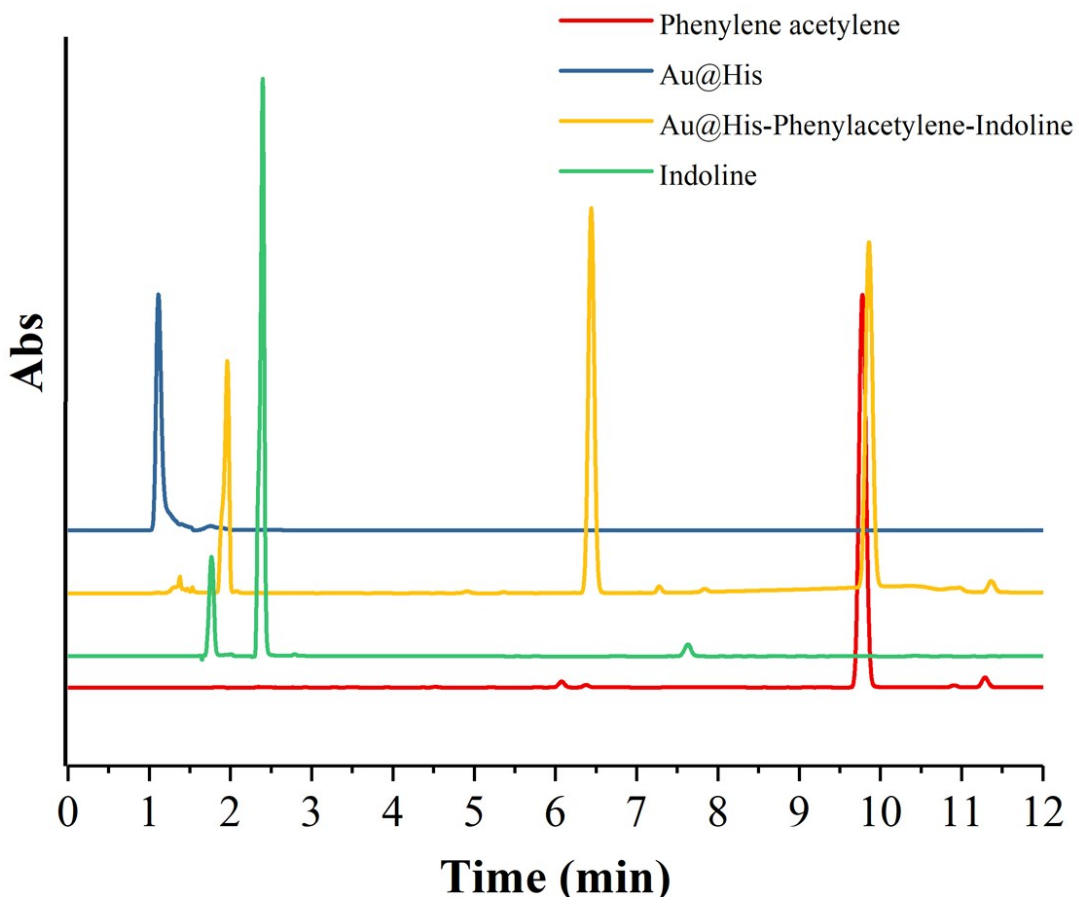

Figure S17 The HPLC chromatogram of the enamine reaction with the phenylacetylene and indoline was obtained under the catalytic activity of Au-$(His)_2$ for a reaction time of 20 min. It has the different retention time of 1.2 min, 2.4 min, 6.5 min, and 9.1 min for the Au-$(His)_2$, indoline, product, and phenylacetylene, respectively.

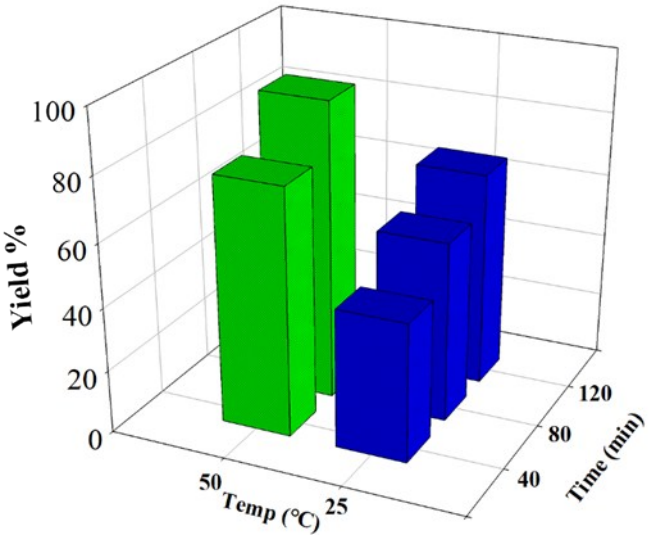

Figure S18 The yields for the different reaction condition (50 ℃ with green color and room temperature with blue color) with the different reaction times (40 min, 80 min, and 120 min)

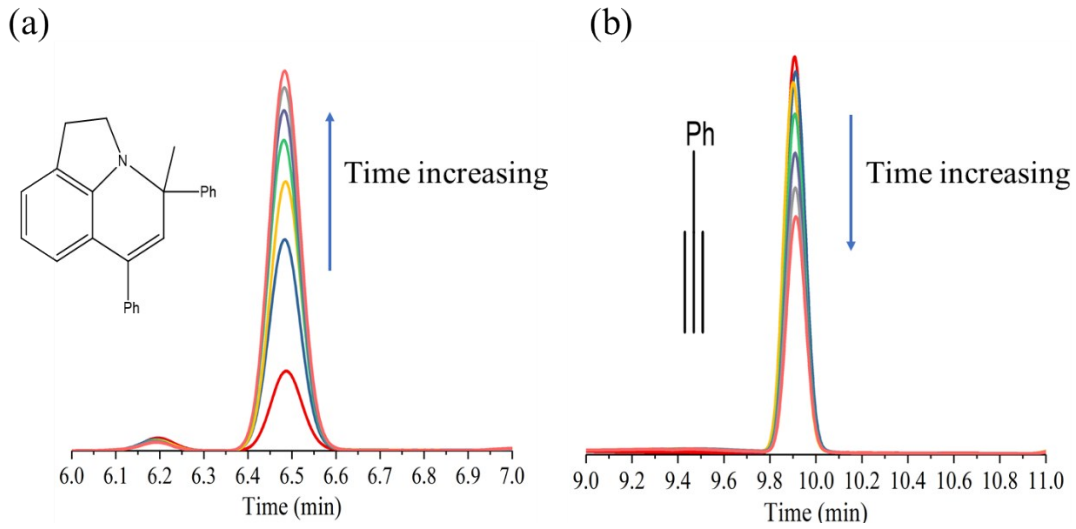

Figure S19 The intensity trend curve of HPLC for (a) the product and (b) the reactant of phenylacetylene in the reaction time range of 40 min.

4,6-Bisphenyl-4-methyl-2,4-dihydro-1*H*-pyrrolo[3,2,1*ij*]quinoline

^{1}H NMR (C_6D_6, 400 MHz) □ = 7.59 (d, *J* = 7.3 Hz, 2H), 7.41 (d, *J* = 5.6 Hz, 2H), 7.23-7.01 (m, 7H), 6.90 (d, *J* = 7.4 Hz, 1H), 6.64 (t, *J* = 7.2 Hz, 1H), 5.37 (s, 1H), 3.16 (dt, *J* = 9.1, 8.7 Hz, 1H), 2.95 (dt, *J* = 8.4, 8.2 Hz), 2.70 (t, *J* = 7.5 Hz), 1.65 (s) ppm. **^{13}C NMR (C_6D_6, 101 MHz)** □ = 148.3, 145.3, 138.4, 134.1, 130.1, 128.4, 128.9, 128.5, 128.1, 127.0, 126.6, 126.0, 124.9, 123.0, 117.1, 116.7, 61.0, 46.8, 28.1, 23.5 ppm. **GC-MS** (M^+ = 323); Anal. Calcd for $C_{24}H_{21}N$: C, 89.13; H, 6.54. Found C, 88.64; H, 6.82

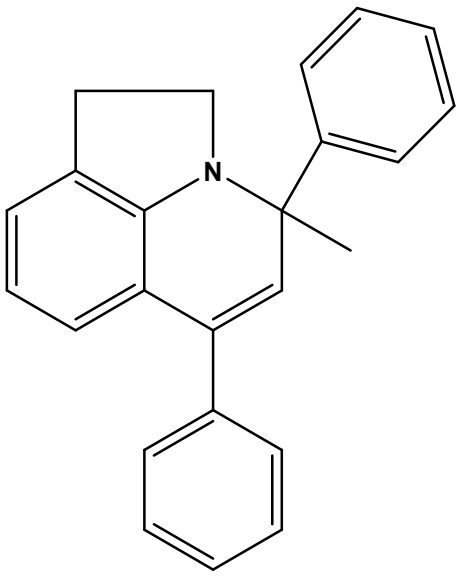

Figure S20 The ^{1}H-NMR and GC-MS results and the structure of product of 4,6-Bisphenyl-4-methyl-2,4-dihydro-1*H*-pyrrolo[3,2,1*ij*] quinoline

(a) 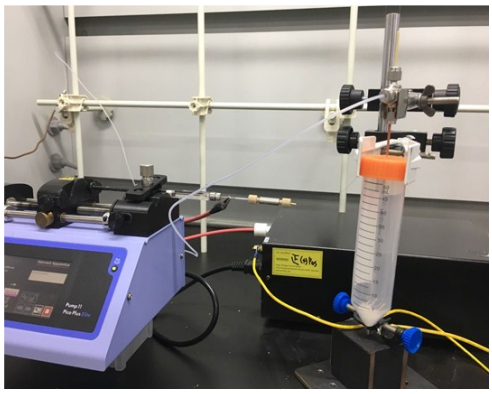 (b) 

Figure S21 (a) The setup of offline homemade-ESSI for collection of Au-$(His)_2$ and (b) the bulk reaction *via* the catalytic activity of Au-$(His)_2$ under stirring.

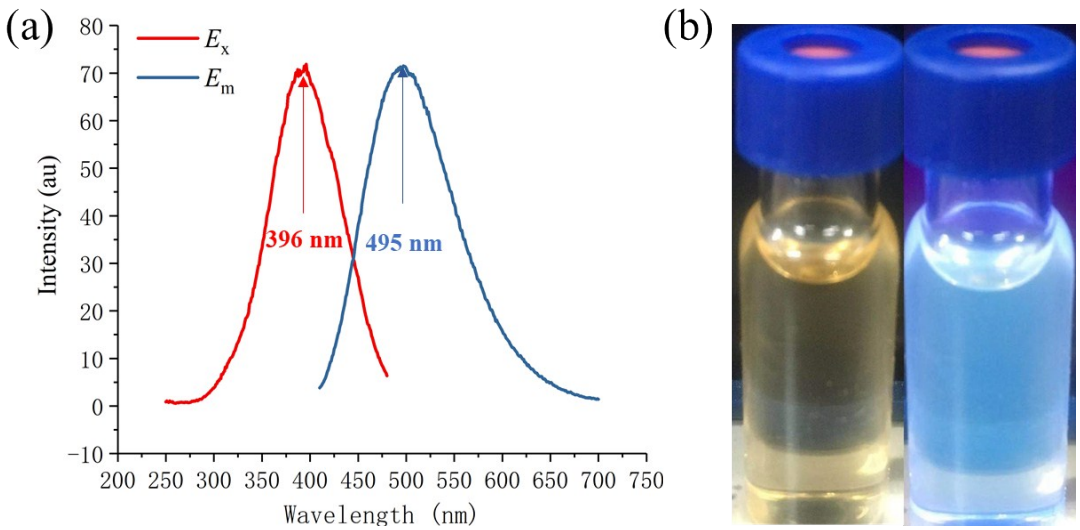

Figure S22. The fluorescence Spectra of Au-$(His)_2$ Complex *via* the microdroplet reaction of histidine (30 mM) and $HAuCl_4$ (10 mM) with the E_x and E_m of 396 nm and 495 nm, respectively (a and b).

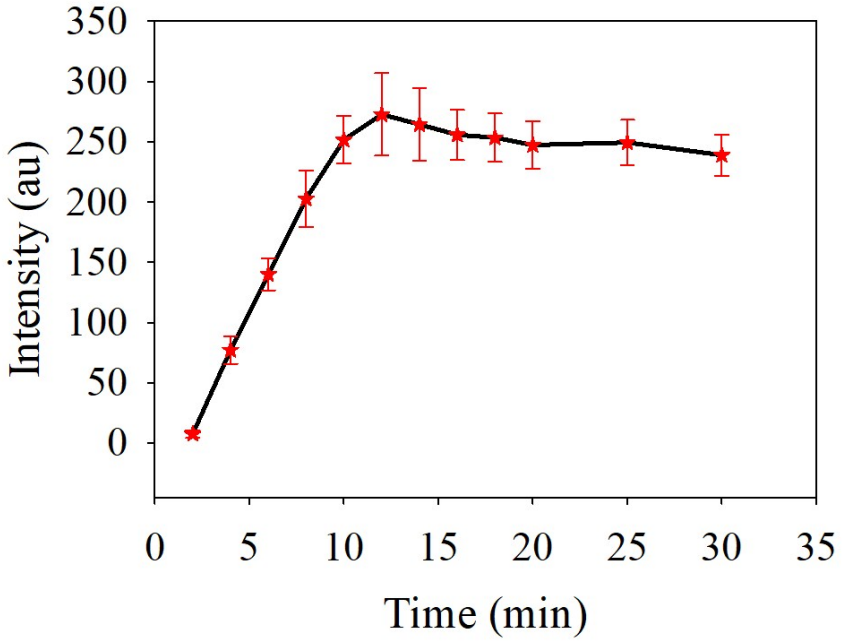

Figure S23 The fluorescence intensity curve of Au-$(His)_2$ *via* the UN microdroplet reaction of histidine (30 mM) and $HAuCl_4$ (10 mM) for different reaction times.

3. References

1. Y. Negishi, K. Nobusada, and T. Tsukuda, *J Am Chem Soc*, 2005, **127**, 5261-5270.

2. L. Challier, R. Miranda-Castro, D. Marchal, V. Noe，F. Mavre, and B. Limoges， J. Am. Chem. Soc., 2013, **135**, 14215-14228.

3. J. Ruiz and B.F. Perandones，*J Am Chem Soc*, 2007, **129**, 9298-9299.